J Mater Sci (2010) 45:566–569
DOI 10.1007/s10853-009-4047-x

LETTER

Solution-processed organic field-effect transistors patterned by self-assembled monolayers of octadecyltrichlorosilane and phenyltrichlorosilane

Sung-Jin Kim · Kyungsun Ryu · Seung Wook Chang

Received: 16 September 2009 / Accepted: 17 November 2009 / Published online: 1 December 2009

Organic field-effect transistors (OFETs) have gathered great interest in the last decade because of the potential application to low-cost printed electronics and large-area flexible electronic devices [1, 2]. In particular, fabrication techniques such as ink-jet printing, micro-contact printing, and roll-to-roll processing of polymeric functional materials enable the realization of high performance solution-processed OFETs [3–7]. Recently, many groups have observed that the performance of OFETs can be significantly improved by treating the insulator surface with self-assembled monolayer (SAMs) such as octadecyltrichlorosilane (OTS) [8–10], fluoroalkyltrichlorosilane (FTS) [11], and phenyltrichlorosiane (PTCS) [12–14]. SAMs modification of dielectric surface provides emerging applications for semiconductor molecules to achieve optimum molecular ordering and crystallinity for charge carrier transport. For example, SAMs can enhance a wettability of the gate dielectric interface by presenting hydrophobic molecules on a substrate. Thus, pentacene and rubrene molecules with OTS SAMs can be sufficiently thick and highly packed crystalline film [12].

However, for the solution-processed OFET devices with polymeric organic semiconductors dissolved in polar solvents, the coating uniformity and coverage are in trouble due to deweting of soluble organic semiconducting layers on the hydrophobic SAMs. Therefore, a novel SAMs manipulation for soluble semiconducting polymers, which meets the requirements of high constancy polymeric thin-films, is needed in order to develop OFETs with high device performance. In this work, we present new solution-processed OFETs having the strong steric effect and intermolecular force between SAMs and the fused ring aromatic based polymeric semiconductor. The devices have a good film coverage for the soluble organic semiconductor, which in turn improves a high current on/off after OTS and PTCS SAMs treatment because of highly packed crystalline films and drastic decrease of peripheral leakage path.

In general, a hydrophobic surface can be easily obtained by using a long methyl group based OTS SAMs. PTCS SAMs are wettable for organic solvents and high affinity to polymeric semiconductor to improve the device stability. Figure 1a, b shows molecular structures of OTS SAMs with a methyl group at the end of a long methylene chain ($C_{18}H_{37}$) and PTCS SAMs with a phenyl group (C_6H_5). The different surface energy results from these head group of SAMs. It is found that the hydrophobicity on the surface of SAMs can be analyzed from the contact angle measurement shown in Fig. 1c, d. Compared to the hydrophobic OTS SAMs, the PTCS SAMs have high surface energy, providing better interaction with the fused-ring aromatic organic semiconductor [12, 13].

Figure 2 shows the optical micrograph of poly(9-9-dioctylfluorene-*co*-bithiophene) (F8T2) layer on OTS and PTCS SAMs. The soluble semiconducting polymer of the F8T2 presents unusual surface wettability for OTS and PTCS SAMs. Figure 2a shows some islands aggregated with the soluble semiconducting polymers on the surface of the hydrophobic OTS SAMS. On the contrary, the F8T2 layer on the hydrophilic PTCS SAMs, as indicated in

S.-J. Kim (✉)
Center for Organic Photonics and Electronics (COPE)
and School of Electrical and Computer Engineering, Georgia
Institute of Technology, Atlanta, GA 30332, USA
e-mail: sjkim@gatech.edu

K. Ryu
Department of Electrical Engineering, Columbia University,
New York, NY 10027, USA

S. W. Chang
Samsung Mobile Display Co., Ltd, San 24, Yongin City,
Gyenggi-Do, Korea

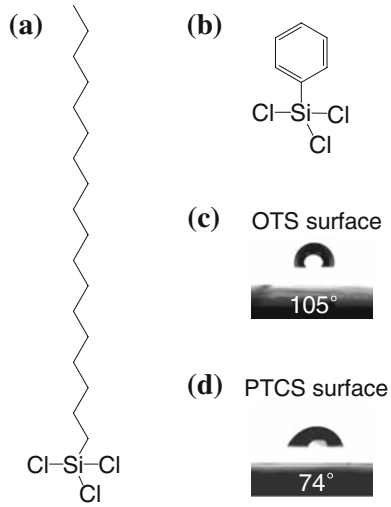

Fig. 1 Molecular structures of **a** OTS and **b** PTCS. Contact angle on the surface of **c** OTS and **d** PTCS

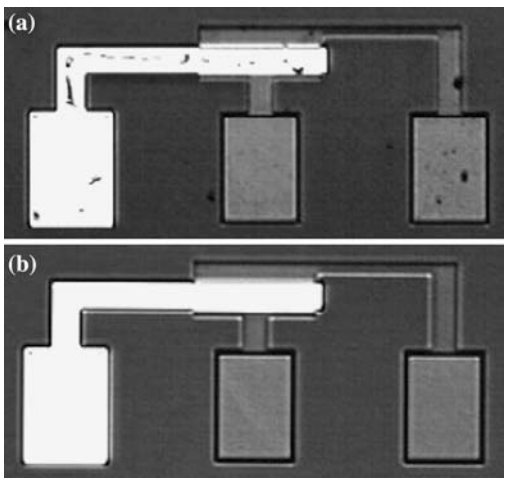

Fig. 2 Optical micrograph of 1 wt% F8T2 layer dissolved in *p*-xylene on **a** OTS and **b** PTCS SAMs

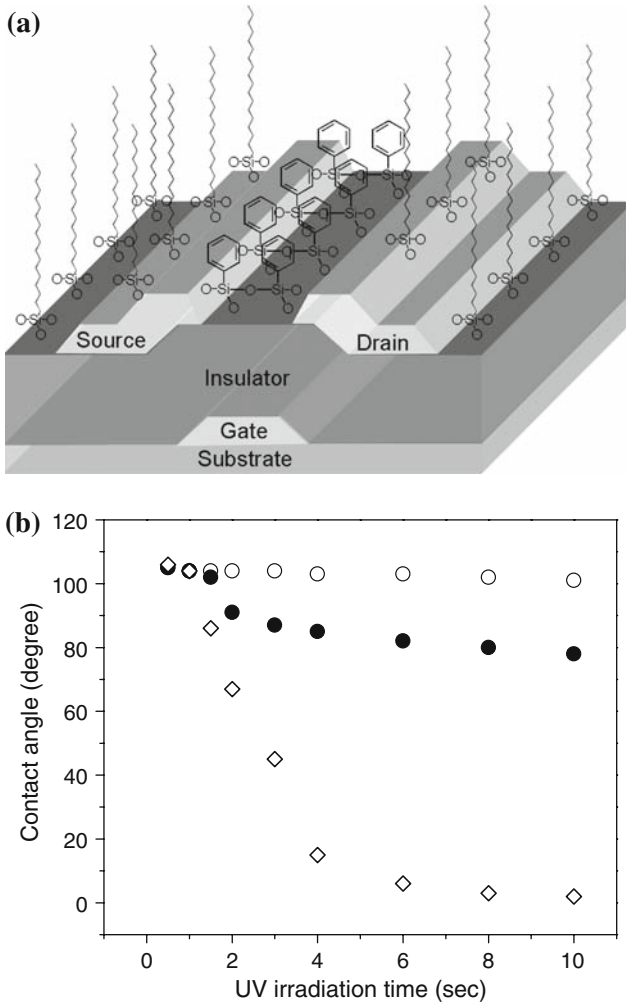

Fig. 3 **a** Schematic cross section of the OFET with a p-type polymeric semiconductor thin film coated on OTS and PTCS SAMs-modified gate insulator. **b** The water drop contact angle for OTS SAMs as a function of the UV irradiation time. UV irradiation (248 nm) density is at 300 mW/cm^2 (*open circle*), 600 mW/cm^2 (*filled circle*), and 900 mW/cm^2 (*diamond*)

Fig. 2b, covers whole area without any defects and pinholes. As the phenyl groups of PTCS SAMs have the strong steric effect and inter-molecular force, the film coverage for the polymeric F8T2 layer on OTS SAMs is lower than that of PTCS SAMs. Even though hydrophobic SAMs performs the semiconductor molecules to assemble as the edge-on orientations and the higher π–π stacking controlling the threshold voltage and achieving better device performance [15], it has problems with the film morphology and the coating uniformity for solution-processed OFETs. Therefore, some researchers have been recently explored a decent tradeoff between wettability and surface energy for an advantage in solution-processed OFETs using by phenyl-terminated SAMs [13].

Figure 3a shows the schematic diagram of the solution-processed OFETs using SAMs with different head groups of methyl and phenyl. The device architecture is a bottom contact geometry with a deposited MoW gate on a glass substrate, a SiO_2 insulator with a thickness of 100 nm, indium tin oxide source-drain metal electrodes, and a soluble polymeric organic semiconductor of the F8T2 with 1 wt% in *p*-xylene. OTS SAMs were fabricated on the SiO_2 insulator. To simultaneously build up the another PTCS SAMs only on the effective channel region, some OTS SAMs were removed by the UV irradiation through a photomask in the presence of the UV irradiation with a wavelength of 248 nm at about 900 mW/cm^2 for 6–8 s. As the UV irradiation time and intensity (300, 600, and 900 mW/cm^2) are increased, the contact angle of OTS SAMs is changed by 105° to less than 5° as shown in Fig. 3b. On the irradiated OTS SAMs, the head groups of SAMs were destroyed by the high-energy photons and

replaced by OH groups. Subsequently, the substrate was immersed in 1 mM PTCS SAMs. The chemical bonding of OTS SAMs is notably stable and irresponsive to other reaction. However, OH groups on the surface immediately react to the PTCS SAMs on the UV irradiation region. UV irradiation onto the methyl group based hydrophobic region typically induces a photochemical organic reaction which involves discontinuity of Si–O or O–C bonds to develop oxygen radical generation, which can react with aerial oxygen and moisture to form OH groups and modify again with phenyl group SAMs. As a result, two different SAMs on the same insulator layer could be simply fabricated. The phenyl groups in the PTCS SAMs were covered along the effective channel area, providing highly molecularly packed organic semiconductors and better surface morphology without pinholes or defects [12, 13].

The device performances of our fabricated OTFTs with a channel length of 20 μm, a channel width of 300 μm, and a gate dielectric capacitance per unit area of 16.3 nF/cm^2 were measured by using the Keithley 4200 semiconductor characterization system in air at room temperature. Transfer characteristics of the device are shown in Fig. 4. The source-drain current (I_D) in a logarithmic scale is shown against the gate voltage (V_G) at a constant source-drain voltage of $V_D = -30$ V. The measurement was performed under four different conditions such as no treatment, OTS SAMs, PTCS SAMs, and OTS and PTCS SAM structure, respectively. The corresponding current on/off ratios were measured to be

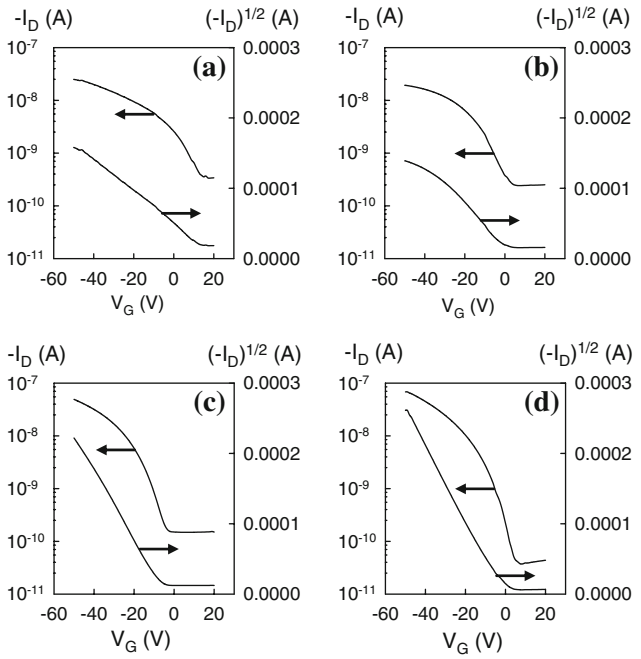

Fig. 4 Transfer characteristics of F8T2 OFET devices grown on different SAMs. Semilogarithmic plot of I_D versus V_G for the devices with **a** no treatment, **b** OTS SAMs, **c** PTCS SAMs, and **d** OTS and PTCS SAM structure

7.4×10^1, 3.3×10^2, 7.9×10^2, and 1.8×10^3. Figure 4b, c clearly shows that the I_D values strongly depend on the SAMs molecules, which is indicating that the surface carrier is substantially modulated by changing the SAMs molecules. The measured field-effect mobility of the solution-processed OFETs using SAMs with different head groups was about 3.3×10^{-4} cm^2/(Vs) in the saturation regime. The field-effect mobility of the device by new SAMs manipulation performs 4–5 times better than the device performance without treatment. This may suggest that further interface and device optimization can lead to increased performance.

Typically, when soluble organic semiconductors are fabricated on our device architecture, the films are more likely to be created on the region of PTCS SAMs with high surface energy rather than that of OTS SAMs with low surface energy. This is expected because low energy hydrophobic surfaces give rise to partial or complete dewetting to the polar solvent dissolving organic semiconductor by intermolecular van der walls forces [16–19]. Therefore, they provide effects of wettabiltiy-based patterning to block the unintentional carrier transport. A current on/off ratio, as we prospected, was improved to 1.8×10^3 after OTS and PTCS SAMs treatment. It is presumably due to the self-organization with high packing density of organic films from the different surface energy and drastic decrease of peripheral leakage path patterned by selective wettaibity [20, 21]. In addition, we found that there was no serious drop of on-current level in the OFETs with OTS and PTCS SAMs through solution-processed technique.

In summary, we have fabricated solution-processed OFETs using SAMs with the different head groups of methyl and phenyl. This new SAMs manipulation for polymeric semiconductors can provide not only the high crystalline thin-film and coating uniformity along a channel area, but also the improved current on/off ratio and field-effect mobility, which allow scaling of the fabrication method to large-area flexible organic electronics while achieving good device uniformity and yield.

Acknowledgements This work was supported by the Korea Research Foundation Grant funded by the Korean Government (KRF-2007-357-D00106).

References

1. Dimitrakopoulos CD, Malenfant PRL (2002) Adv Mater 14:99
2. Ling MM, Bao Z (2004) Chem Mater 16:4824
3. Chabinyc ML, Salleo A (2004) Chem Mater 16:4509
4. Briseno AL, Mannsfeld SCB, Ling MM, Liu S, Tseng RJ, Reese C, Roberts ME, Yang Y, Wudl F, Bao Z (2006) Nature 444:913
5. Chabinyc ML, Salleo A, Wu Y, Liu P, Ong BS, Heeney M, McCulloch I (2004) J Am Chem Soc 126:13928
6. Facchetti A, Yoon M-H, Marks TJ (2006) J Am Chem Soc 128:4928

7. Menard E, Bilhaut L, Zaumseil J, Rogers JA (2004) Langmuir 20:6871
8. Lee HS, Kim DH, Cho JH, Hwang M, Jang Y, Cho K (2008) J Am Chem Soc 130:10556
9. Masuda Y, Kinoshita N, Sato F, Koumoto K (2006) Cryst Growth Des 6:75
10. Seo JH, Chang GS, Wilks RG, Whang CN, Chae KH, Cho S, Yoo K-H, Moewes A (2008) J Phys Chem B 112:16266
11. Calhoun MF, Sanchez J, Olaya D, Gershenson ME, Podzorov V (2008) Nat Mater 7:84
12. Li Y, Wu Y, Ong BS (2006) Macromolecules 39:6521
13. Liu Z, Becerril HA, Roberts ME, Nishi Y, Bao Z (2009) IEEE Trans Electron Device 56:176
14. Oberhoff D, Pernstich KP, Gundlach DJ, Batlogg B (2007) IEEE Trans Electron Device 54:17
15. Umedaa T, Tokito S, Kumaki D (2008) J Appl Phys 101:054517
16. Wang JZ, Zheng ZH, Li HW, Huck WTS, Sirringhaus H (2004) Nat Mater 3:171
17. Kim SH, Choi D, Chung DS, Yang C, Jang J, Park CE, Park S-HK (2008) Appl Phys Lett 93:113306
18. Park SK, Mourey DA, Subramanian S, Anthony JE, Jackson TN (2008) Adv Mater 20:4145
19. Na Y-J, Lee S-W, Choi W, Kim S-J, Lee S-D (2009) Adv Mater 21:537
20. Kim S-J, Ahn T, Suh MC, Yu C-J, Kim D-W, Lee S-D (2005) Jpn J Appl Phys 44:L1109
21. Kim S-J, Beveridge H, Koberstein JT, Kymissis I (2009) J Vac Sci Technol B 27:1057